

Femtosecond laser writing of buried graphitic structures in bulk diamond

M. Neff · T.V. Kononenko · S.M. Pimenov · V. Romano ·
W. Lüthy · V.I. Konov

Received: 29 May 2009 / Accepted: 12 August 2009 / Published online: 2 September 2009
© Springer-Verlag 2009

Abstract Diamond samples are irradiated with 140 fs pulses of 800 nm wavelength. The pulse repetition rate is 1 kHz. In the focal region of the irradiated pulses the diamond is transformed to graphite. The writing of graphitic wires along the incident beam is studied experimentally. A technique to produce buried graphitic wires with constant diameter is described. Diameters can be selected between 1.5 μm and 10 μm . The wire length is up to 680 μm . The writing speed is typically between 1 $\mu\text{m s}^{-1}$ and 30 $\mu\text{m s}^{-1}$.

PACS 61.80.Ba · 79.20.Ds · 81.05.Uw

1 Introduction

It has been shown that diamond samples can be micro structured with fs-laser pulses [1–4]. These experiments showed the appearance of breakdown on the diamond surface as well as in the bulk. With the use of fs-laser pulses thermal conductivity can be neglected and therefore very fine structures can be expected [5]. With Raman spectroscopy it could be shown that the generated structures consist of graphite [3, 6]. Also theoretical studies showed that under the interaction with fs-laser pulses a diamond should undergo a non-equilibrium phase transition from the

metastable sp^3 -bonded diamond to the stable sp^2 -bonded graphite [2, 7–9]. Such micro-structured diamonds are interesting by themselves, but can also be used for practical applications such as optical memories with a storage density comparable to a DVD [10] or for the generation of photonic crystal structures. Another application could be found in the production of diamond photodiodes or in ultra-fast micro-structured electrical high voltage devices [11]. Due to the constant development of the CVD technology that also allows rapid growth [12, 13] synthetic diamond is available in a large product range of desired size shape and price.

Until now, several experiments have been performed which provide information about the nature of these micro-structures as well as power thresholds required to produce breakdown on the diamond surface or in bulk [1–4]. Especially in [3] and [4] it has been shown, however, that repetitive irradiation into the bulk of the diamond sample results not only in a graphitization in the focus of the laser beam but tends to grow towards the incident beam. This continued growth can influence the writing of lateral and longitudinal structures in an undesired way. With the goal to better understand and control the structuring process, in a first step the writing of longitudinal structures has to be studied in more detail. In this paper we compare the continuous growth with stationary focusing with the growth due to a focus in uniform motion towards the incident beam. It is shown that very fine structures close to the optical resolution can be written if the speed of the moving focus is chosen appropriately.

2 Experimental

The experimental setup is shown schematically in Fig. 1. For micro-structuring a mode-locked Ti:sapphire laser (Spectra

M. Neff (✉) · V. Romano · W. Lüthy
Institute of Applied Physics, University of Bern, Sidlerstrasse 5,
3012 Bern, Switzerland
e-mail: martin.neff@iap.unibe.ch
Fax: +41-31-6313765

T.V. Kononenko · S.M. Pimenov · V.I. Konov
Natural Science Center, General Physics Institute,
Vavilov street 38, 119991 Moscow, Russia

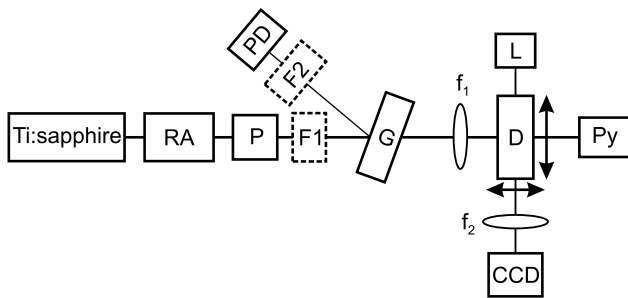


Fig. 1 Experimental arrangement with mode-locked titanium sapphire laser (Ti:sapphire), regenerative amplifier (RA), Pockels cell (P), neutral density Filters (F1 and F2), glass plate (G), photo diode (PD), microscope objectives $20\times$ (f_1), adjustable diamond sample (D), pyroelectric detector (Py), incandescent lamp (L), microscope objective $10\times$ (f_2), and CCD camera (CCD)

Physics Tsunami) operated at 800 nm with 12 nJ pulse energy is used. The output is amplified with a regenerative amplifier (Spitfire Pro) to 1 mJ. The pulse length of the laser system is 140 fs at a repetition rate of 1 kHz. The power irradiated onto the target is adjusted with optical filters. To measure the chosen laser power during the experiment, about 8% of the beam is reflected at a microscopic object plate of a thickness of $150\ \mu\text{m}$ tilted by about 10° to the incident beam. The reflected laser signal is detected with a photodiode (FD-24). To allow monitoring of the interaction from the side of the target, the experiments are performed on monocrystalline diamond samples of $5\ \text{mm} \times 1.5\ \text{mm} \times 0.5\ \text{mm}$. These samples are of optical quality with polished sides. For adjustment and also to produce continuous structures the diamond samples are mounted on a three-dimensional translation stage. The translation stage along the beam direction is motor driven with a velocity down to $1\ \mu\text{m s}^{-1}$. The laser beam is focused into the sample with a $20\times$ microscope objective. The obtained beam diameter at intensity level $1/e$ in the focal plane is measured to be $2.3\ \mu\text{m}$ using the technique of Liu [14]. The generation of the graphite structures is observed perpendicularly to the laser beam. With a microscope objective ($10\times$) of long working distance the target is imaged onto a CCD camera. The working distance is sufficient to image the full lateral dimension of the diamond sample of 5 mm. For illumination the transmitted light of an incandescent lamp is used. Behind the sample the energy of the laser pulses is measured with a pyroelectric detector (Spectra Physics 407A). With the sample removed this detector is used to calibrate the photodiode.

3 Results

In a first experiment the continuous growth rate with a stationary focal plane of the incident laser beam is measured. The focus of the incident beam is set at the rear surface of

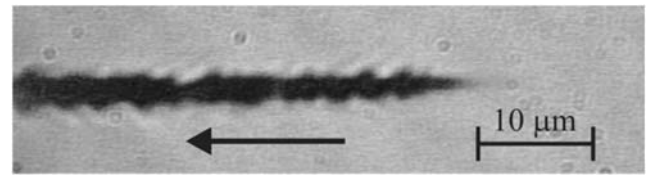


Fig. 2 Continuous graphitization at an incident power of $210\ \mu\text{W}$. The arrow indicates the direction of irradiation. The left border of the figure coincides with the rear surface. With continued irradiation the graphitized region grows in the direction opposite to the arrow

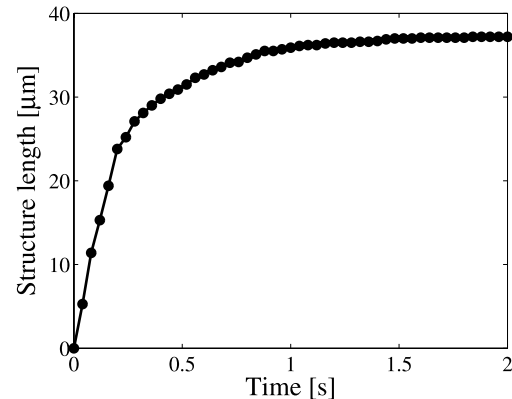


Fig. 3 Length of the structure produced with a power of $210\ \mu\text{W}$ as a function of time

the diamond sample. With respect to the bulk, the graphitization threshold at the surface is essentially lower. The duration of the laser irradiation is selected with a shutter (Pockels cell P). With an average power of $210\ \mu\text{W}$ that is close to the damage threshold the initial breakdown occurs at the rear surface. After this first lesion the graphitized structure grows towards the incident laser beam. This continuous growth arises due to the high absorption in graphite allowing also lower laser intensities to reach the interaction threshold. The graphitized region after 20 seconds of irradiation is shown in Fig. 2.

The temporal development of the graphite trace is recorded with a frame rate of 25 images per second. Figure 3 shows the growth rate for the first 50 frames. In these 2 seconds after the appearance of the breakdown nearly the whole structure is generated. In the following 18 seconds the length of the graphitization increased only by about $2\ \mu\text{m}$.

From Fig. 2 it is seen that the graphitized region has a conical shape. The temporal development of the structure diameter during the growth process is determined. In each of the 53 first frames only the new generated part of the structure is analyzed. There the diameter is measured at the thickest part at the front end at FWHM of the grey value. Since the shape of the structure front changes somewhat in each frame the measured diameters scatter but still a linear decrease of the diameter as a function of time can be seen (cf. Fig. 4)

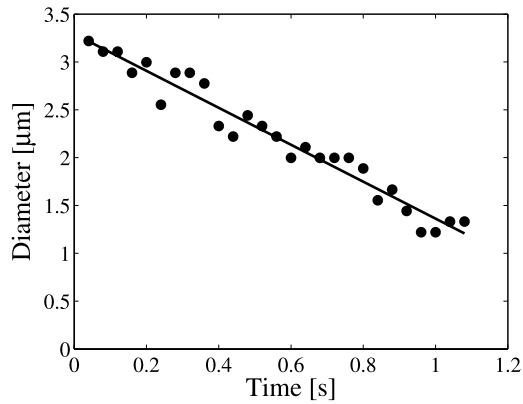


Fig. 4 Diameter of the structure produced with a power of 210 μW as a function of time. The diameter is measured at FWHM of the grey values. The trend line is a linear approximation

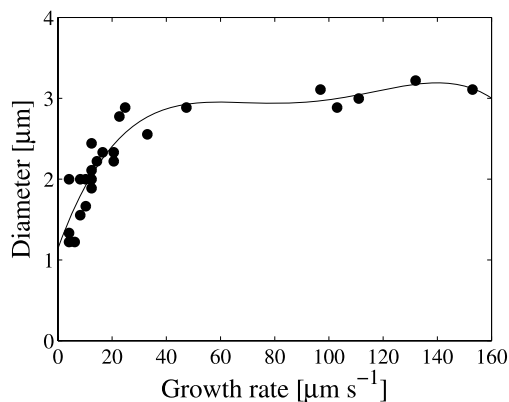


Fig. 5 Diameter of the structure produced with a power of 210 μW as a function of growth rate. The trend line is a polynomial of 4th order

A comparison of Figs. 3 and 4 allows determining the diameter of the structures as a function of the growth rate. The result is shown in Fig. 5.

The same experiments have also been performed with a power of 1.53 mW. A sequence of frames is shown in Fig. 6.

From the figure it is seen that damage starts with a series of small lesions. The power of the laser is high enough to produce a graphitization even 65 μm away from the surface. This graphitization shadows the other lesions from the laser beam and continues to grow towards the incident beam.

The length of the graphitized region as a function of time is shown in Fig. 7. In view of the first 65 μm that are generated at the very beginning of the irradiation, the structure length is only evaluated between 60 μm and 100 μm .

In a second experiment the focus is positioned behind the surface so that no interaction occurs. Then the focus is moved with constant speed towards the irradiating beam. When the intensity is sufficient to start the interaction, the diameter of the graphitization depends on the constant speed in the same way as the cone diameter on the growth rate of

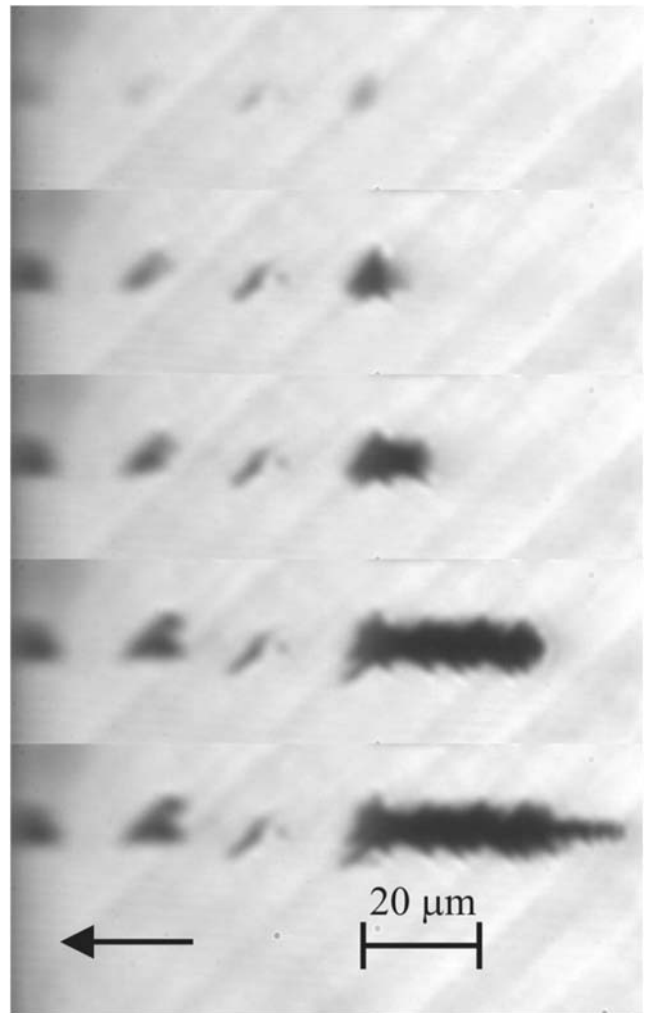


Fig. 6 Development of the graphitization with an irradiated power of 1.53 mW. The left border of the picture coincides with the rear surface. The arrow shows the direction of the irradiated light. The different frames (from top to bottom) are taken at 40 ms, 80 ms, 120 ms, 1 s and 2.76 s

Fig. 5. This causes smaller diameters for lower speed. Experimental traces of graphite produced with different speed are shown in Fig. 8.

With a laser power of 210 μW the graphitization threshold is only reached in a small area with a diameter comparable to the focus diameter. Therefore the interaction region is well localized and not spread over a wide area. This allows writing of structures with a constant diameter. The diameter of the produced structure can be chosen by adjusting the writing velocity.

The same experiment was also performed with 1.53 mW. The result is shown in Fig. 9.

From Fig. 6 it is seen that with a laser power of 1.53 mW breakdowns occur not only in the focal plane as it happens with 210 μW . The threshold to allow a breakdown is reached in an area of 65 μm around the focal plane. The occurrence of the breakdown is then not controllable and depends on the

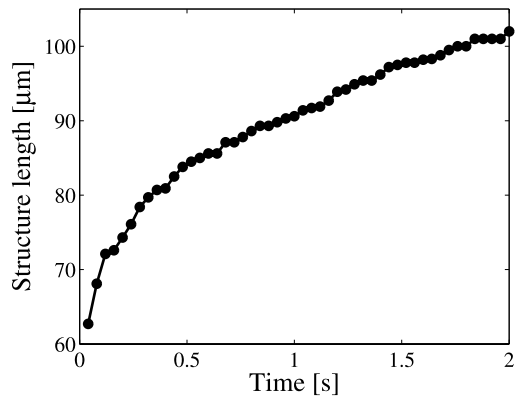


Fig. 7 Length of the structure produced with a power of 1.53 mW as a function of time

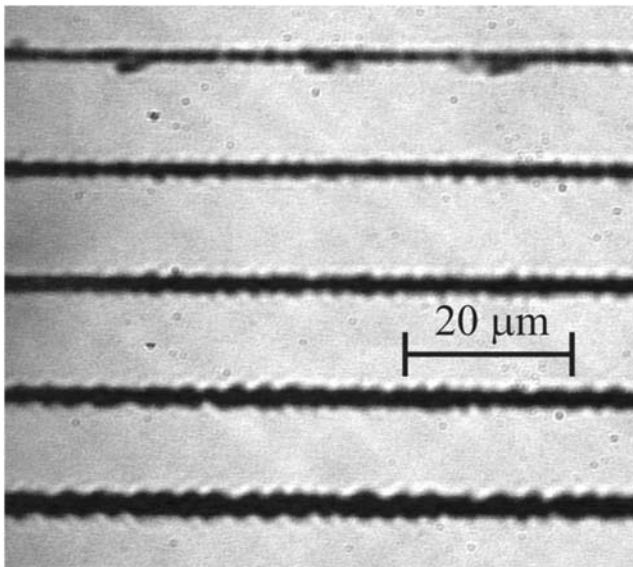


Fig. 8 Graphitized traces written with 210 μW with speeds of (from top to bottom) $1 \mu\text{m s}^{-1}$, $3 \mu\text{m s}^{-1}$, $5 \mu\text{m s}^{-1}$, $10 \mu\text{m s}^{-1}$ and $30 \mu\text{m s}^{-1}$. The width of the traces is about 1.5 μm , 2 μm , 2.5 μm , 3 μm , and 3.5 μm respectively. The length of the traces was up to 680 μm in a correspondingly thicker sample

local irregularities of the bulk. Consequently also in Fig. 9 no regular traces are written. Due to this unpredictable appearance of breakdowns the traces tend to be interrupted. These new spots of graphitization shadow the preliminarily generated traces which therefore cannot grow any further.

Independent from speed in the range of $30 \mu\text{m s}^{-1}$ to $100 \mu\text{m s}^{-1}$ all the traces have about 10 μm width. Only for growth rates lower than $30 \mu\text{m s}^{-1}$ an essential reduction of the diameter can be observed (cf. Figs. 6 and 7). The same relation of growth rate and diameter can be seen in Fig. 5 which is valid for a laser power of 210 μW . The diameter of the continuous growth is rather constant for growth rates between $25 \mu\text{m s}^{-1}$ and $160 \mu\text{m s}^{-1}$. Only for growth rates lower than $25 \mu\text{m s}^{-1}$ smaller diameters can be achieved.

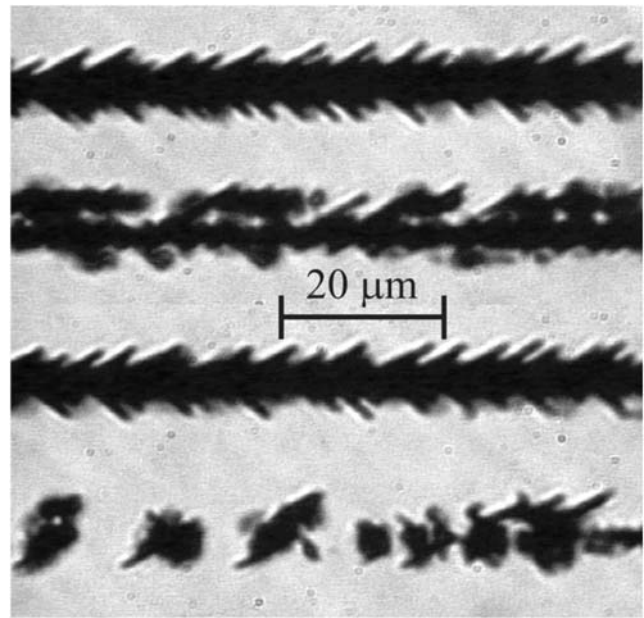


Fig. 9 Graphitized traces written with 1.53 mW with speeds of (from top to bottom) $30 \mu\text{m s}^{-1}$, $30 \mu\text{m s}^{-1}$, $50 \mu\text{m s}^{-1}$, and $100 \mu\text{m s}^{-1}$. The width of all the traces is about 10 μm

We assume that shadowing is also responsible for the feather-like shape of the traces in Fig. 9. The occurrence of a primary modulation of the written trace is based on instabilities described in [15]. The crucial parameters that can lead to instabilities are listed in chapter 28.3 of [15]. Due to these instabilities the graphitization does not occur in a smooth line but rather in a chain of bumps as they can be seen in Fig. 8. These bumps can continue to grow at their illuminated side until they are shadowed by a next bump in growth direction. In Fig. 8 these feathers are less pronounced since graphitization is limited to the focal region.

From these findings we conclude that writing of longitudinal structures is best controlled with a laser power that is only slightly above the threshold for graphitization. This assures that the interaction only occurs in the focal region. Under the same conditions it should also be possible to write lateral structures. Efforts to experimentally verify this lateral graphitization are in progress.

4 Conclusion

Monocrystalline diamond samples were irradiated with 140 fs pulses of 800 nm wavelength. The pulse repetition rate was 1 kHz. In the focal region of the irradiated pulses the diamond is transformed to graphite. The writing of graphitic wires along the incident beam was studied experimentally. A technique to produce buried graphitic wires with constant diameter has been described. Diameters can be selected between 1.5 μm and 10 μm . The length of the trace

was up to 680 μm . The writing speed is typically between 1 $\mu\text{m s}^{-1}$ and 30 $\mu\text{m s}^{-1}$. It is shown that regular traces with small diameter can be produced with a laser power that is only slightly above the interaction threshold and low scanning speed close to 1 $\mu\text{m s}^{-1}$.

Acknowledgements We thank T. Feurer for helpful discussions. This work was supported in part by the Swiss National Science Foundation under contract No. IB7420-110873/1 and the Russian Foundation for Basic Research under project No. 08-02-12082

References

1. C.Z. Wang, K.M. Ho, M.D. Shirk, P.A. Molian, Laser-induced graphitization on a diamond (111) surface. *Phys. Rev. Lett.* **85**, 4092–4095 (2000)
2. V.N. Strekalov, V.I. Konov, V.V. Kononenko, S.M. Pimenov, Early stages of laser graphitization of diamond. *Appl. Phys. A* **76**, 603–607 (2003)
3. T.V. Kononenko, M. Meier, M.S. Komlenok, S.M. Pimenov, V. Romano, V.P. Pashinin, V.I. Konov, Microstructuring of diamond bulk by IR femtosecond laser pulses. *Appl. Phys. A* **90**, 645–651 (2008)
4. T.V. Kononenko, M.S. Komlenok, V.P. Pashinin, S.M. Pimenov, V.I. Konov, M. Neff, V. Romano, W. Lüthy, Femtosecond laser microstructuring in the bulk of diamond. *Diam. Relat. Mater.* **18**, 169–199 (2009)
5. S. Gloor, W. Lüthy, H.P. Weber, Submicron laser writing on diamond. *Diam. Relat. Mater.* **8**, 1853–1856 (1999)
6. Q. Wu, L. Yu, Y. Ma, Y. Liao, R. Fang, L. Zhang, X. Chen, K. Wang, Raman investigation of amorphous carbon in diamond film treated by laser. *J. Appl. Phys.* **93**, 94–100 (2003)
7. H.O. Jeschke, M.E. Garcia, K.H. Bennemann, Theory for laser-induced ultrafast phase transitions in carbon. *Appl. Phys. A* **69**(Suppl.), 49–53 (1999)
8. H.O. Jeschke, M.E. Garcia, K.H. Bennemann, Microscopic analysis of the laser-induced femtosecond graphitization of diamond. *Phys. Rev. B* **60**, R3701–R3704 (1999)
9. V.N. Strekalov, Graphitization of diamond stimulated by electron-hole recombination. *Appl. Phys. A* **80**, 1061–1066 (2005)
10. J. Qiu, K. Miura, T. Suzuki, T. Mitsuyu, K. Hirao, Permanent photoreduction of Sm^{3+} to Sm^{2+} inside a sodium aluminoborate glass by an infrared femtosecond pulsed laser. *Appl. Phys. Lett.* **74**, 10–12 (1999)
11. S.V. Garnov, S.M. Klimentov, A.I. Ritus, S.M. Pimenov, V.V. Konov, S. Gloor, W. Lüthy, H.P. Weber, Ultrafast electronic processes in natural and CVD diamonds. *Diam. Films Technol.* **8**, 369–380 (1998)
12. V.I. Konov, A.M. Prokhorov, S.A. Uglov, A.P. Bolshakov, I.A. Leontiev, F. Dausinger, H. Hügel, B. Angstenberger, G. Sepold, S. Metev, CO_2 laser-induced plasma CVD synthesis of diamond. *Appl. Phys. A* **66**, 575–578 (1998)
13. Y. Meng, C. Yan, J. Lai, S. Krasnicki, H. Shu, T. Yu, Q. Liang, H. Mao, R.J. Hemley, Enhanced optical properties of chemical vapour deposited single crystal diamond by low-pressure/high-temperature annealing. *Proc. Natl. Acad. Sci.* **105**, 17620–17625 (2008)
14. J.M. Liu, Simple technique for measurements of pulsed Gaussian-beam spot sizes. *Opt. Lett.* **7**, 196–198 (1982)
15. D. Bäuerle, *Laser Processing and Chemistry*, 3rd edn. (Springer, Berlin, 2000)